Structuring efficient photocatalysts into bespoke fiber shaped systems for applied water treatment

Theodorakopoulos G.[1,2,*], Romanos G.[2], Katsaros F.[2], Papageorgiou S.[2], Falaras P.[2], Kontos A.[2], Beazi-Katsioti M.[1]

[1]School of Chemical Engineering, National Technical University of Athens, 9 Heroon Polytechniou Street, 15780 Zografou, Athens, Greece

[2]Institute of Nanoscience and Nanotechnology, N.C.S.R. "Demokritos", 15310 Ag. Paraskevi, Athens, Greece

*corresponding author: George Theodorakopoulos: e-mail: g.theodorakopoulos@inn.demokritos.gr

Abstract

In this study structured photocatalytic systems were successfully developed by a facile method. Polymeric (Alginate) molds, settled the basis in order to effectively disperse and stabilize nanoparticles of an efficient, copper augmented photocatalyst (Degussa P25), which after removal of the polymer by a pyrolytic or calcination-sintering procedure, were shaped in the form of all-ceramic hollow fibers (HFs) with enhanced photocatalytic and mechanical properties and excellent resistance to attrition. The structural and morphological properties have been studied using LN_2 porosimetry, XRD, SEM and Raman spectroscopy. The experimental campaign for elucidating the photocatalytic performance encompassed batch experiments, where the abatement of a prototype organic pollutant (Methyl Orange) was investigated in the dark and under UV irradiation. The obtained performance was benchmarked against that of a prototype photocatalyst implemented in slurry or thin film reactors. The role and the contribution of zero-valent Cu nanoparticles in the photocatalytic mechanism, as well as of carbon residues from the pyrolytic procedure, were also examined.

Keywords: Photocatalysis; Alginate; Titania; Batch reactor; MO degradation

1. Introduction

The use of photocatalysts in powder form has presented many drawbacks, including the difficult separation of the catalyst from the treated effluent and the non-effective irradiation of the dispersed particles in the photocatalytic slurry (Thiruvenkatachari et al., 2008) with significant capital and operational costs. Recent studies focus on the effective stabilization of the photocatalysts by embedding the photocatalytic particles into the matrix of transparent polymers, which are predominantly structured in the form of fibers and beads and are usually characterized by asymmetry in their pore structure. The very recently conceptualized processes of photocatalytic filtration and photocatalytic bed fluidization (Yilleng et al., 2018) render the fiber and bead shaped photocatalytic systems very promising candidates for future implementation in water purification technologies. However, the porous polymer matrices that envelope the photocatalyst may adversely affect the performance of the photocatalytic process, mostly due to diffusion limitations of the involved polymers hydrophobicity (i.e. PVDF, Hou et al., 2009). Most importantly, the life time of the polymer may be significantly shortened under the conditions of continuous UV irradiation and the oxidative action of the photocatalyst (Yousif et al., 2013). Hence, all recently applied methodologies and state of the art technologies, employ a final stage of calcination/sintering that removes the polymer, resulting in all-ceramic structures with mechanical stability and resistance to attrition.

In this work, alginate was used as the template of photocatalytic systems in the form of all-ceramic hollow fibers (HFs). The optimum formulation has been defined and different sintering temperatures and times were evaluated. The effect of residual carbon from the pyrolytic-sintering procedure, on the stability and photocatalytic performance was also elucidated and discussed. Alginates metal ion sorbing capacity (Papageorgiou et al, 2006) was exploited in order to decorate the photocatalyst with copper nanoparticles and enhance the photocatalytic activity. The photocatalytic performance was evaluated in batch mode experiments under near-UV irradiation, with methyl orange (MO) selected as the model pollutant. It was found that the developed all-ceramic materials are photo-catalytically active. Moreover, the copper decorated all-ceramic HFs exhibited the highest MO adsorption and photocatalytic degradation performance due to the synergistic effect of copper nanoparticles.

2. Results-Conclusions

2.1. Results

Liquid N_2 porosimetry at 77 K was applied to elucidate the pore structural and textural properties of the freshly prepared all-ceramic HFs. The samples exhibit type II N_2 adsorption/desorption isotherms with a sharp capillary condensation step at high relative pressure of $P/P_0 > 0.97$, which is a characteristic of materials containing large mesopores and macropores. The rigid structure and

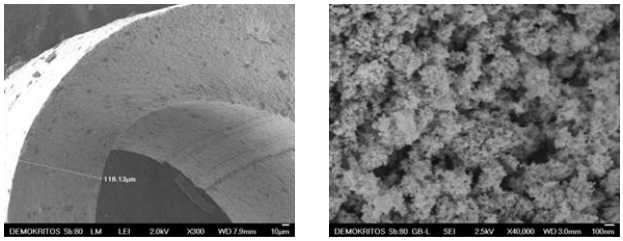

Figure 1. SEM images of cross section and internal surface of sample T6

proper shaping of the pyrolysis derived all-ceramic HFs is confirmed by the SEM images (Figure 1). The XRD patterns confirm the existence of anatase and rutile, the relative ratio of which depends, mainly, on heat treatment conditions of samples and the presence of metallic copper in sample T6. Furthermore, Raman spectroscopy was used to confirm the various phases of titania, as well as of carbon residuals, which display low I_D/I_G ratio, due to the existence of defects in the graphitic structure.

For the examination of the photocatalytic efficiency, two runs were performed using O_2 bubbled and He sparged MO solutions, at the same concentration. In both cases, the results showed the following ranking of the photocatalytic efficiency, T6 > T2 > T4 (Figure 2).

Sample T6 exhibited by far the best photocatalytic efficiency compared to the other pyrolysis derived samples T2 and T4 and reached MO rejection performances of 62.3% and 72.4% in the oxygen saturated and oxygen depleted solutions, respectively. Amongst the causes of the enhanced effectiveness, is definitely the higher MO adsorption capacity of the copper decorated all-ceramic HFs (T6) as compared to the non-decorated ones (T2, T4). Accordingly, the higher photocatalytic efficiency can be explained on the grounds of the synergistic effect of adsorption. Nanoparticles of zero-valent copper not only augment the surface texture and pore volume properties of sample T6, but also have the potential to offer a large population of active centers for MO adsorption. Despite that the synergistic effects of NPs in photocatalysis are evidently related to the higher concentration of the pollutant in the vicinity of the photocatalyst, as well as to the action of metal NPs as a sink of photogenerated electrons that inhibits electron-hole recombination, the capacity of zero valent copper nanoparticles to trigger the reducing path of photocatalysis should also be considered. From this perspective, the electrons photogenerated in the semiconductor migrate to its surface and after being accepted by the metal NPs coupled to TiO_2, they are shuttled to the adsorbed MO molecules, causing the reductive cleavage of the azo group. Thus, the MO molecules accept electrons from the Cu NPs and transform into transitional products, when they are combined with H^+. It can be clearly noticed that under the same possible conditions, the photocatalytic efficiency of HFs (with low light intensity) is approximately of the same level or even higher than the literature work (Andronic et al., 2007).

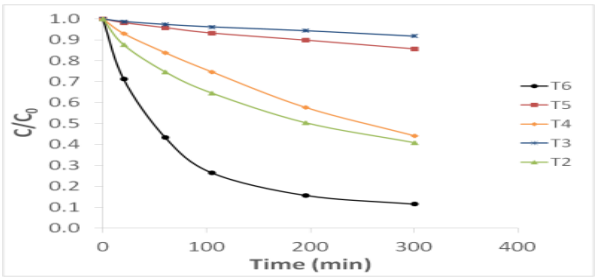

Figure 2. Comparison of the kinetics of MO degradation between all HF samples at the concentration of 6.3 ppm

2.2. Conclusions

In this work, a process that yields shaped photocatalytic systems in the form of all-ceramic HFs has been developed. Tuning of the experimental parameters was carried out aiming to optimize the fibers' properties, mainly in terms of mechanical stability, resistance to attrition and photocatalytic performance. Ceramic hollow fibers display compact structure with rough outer structure, with bimodal porosity: mesoporous due to titania nanoparticles and macroporous due to fiber formation. The addition of copper in the initial stage of the process leads to the creation of highly dispersed metallic copper nanoparticles in the surface of the photocatalyst. The relative ratio of anatase and rutile depends mainly on heat treatment conditions. In conclusion, the immobilized photocatalysts exhibit enhanced photocatalytic and mechanical properties and excellent resistance to attrition, while the incorporation of copper nanoparticles increases significantly the photocatalytic activity. Fibers' dynamic flow experiments are underway to validate the feasibility of their use in industrial processes.

References

Thiruvenkatachari R., Vigneswaran S. and Moon I.S. (2008), A review on UV/TiO_2 photocatalytic oxidation process, *Korean Journal of Chemical Engineering*, **25**, 64-72.

Yilleng M.T., Gimba E.C., Ndukwe G.I., Bugaje I.M., Rooney D.W. and Manyar H.G. (2018), Batch to continuous photocatalytic degradation of phenol using TiO_2 and Au-Pd nanoparticles supported on TiO_2, *Journal of Environmental Chemical Engineering*, **6**, 6382-6389.

Hou D., Wang J., Qu D., Luan Z. and Ren X. (2009), Fabrication and characterization of hydrophobic PVDF hollow fiber membranes for desalination through direct contact membrane distillation, *Separation and Purification Technology*, **69**, 78-86.

Yousif E. and Haddad R. (2013), Photodegradation and photostabilization of polymers, especially polystyrene: review, *SpringerPlus*, **2**, 398-429.

Papageorgiou S.K., Katsaros F.K., Kouvelos E.P., Nolan J.W., Deit H.L. and Kanellopoulos N.K. (2006), Heavy metal sorption by calcium alginate beads from Laminaria digitata, *Journal of Hazardous Materials*, **137**, 1765-1772.

Andronic L. and Duta A. (2007), TiO_2 thin films for dyes photodegradation, *Thin Solid Films*, **515**, 6294-6297.